Time evolution of electron structure in femtosecond heated warm dense molybdenum

F. Dorchies,[1,*] V. Recoules,[2] J. Bouchet,[2] C. Fourment,[1] P. M. Leguay,[1] B. I. Cho,[3] K. Engelhorn,[4] M. Nakatsutsumi,[5] C. Ozkan,[5] T. Tschentscher,[5] M. Harmand,[6] S. Toleikis,[6] M. Störmer,[7] E. Galtier,[8] H. J. Lee,[8] B. Nagler,[8] P. A. Heimann,[8] and J. Gaudin[1]

[1]*Université de Bordeaux, CNRS, CEA, CELIA (Centre Lasers Intenses et Applications), UMR 5107, F-33400 Talence, France*

[2]*CEA-DAM-DIF, F-91297 Arpajon, France*

[3]*Department of Physics and Photon Science, Gwangju Institute of Science and Technology (GIST), Gwangju, Korea*

[4]*Lawrence Berkeley National Laboratory, Berkeley, California 94720, USA*

[5]*European XFEL, Hamburg, Germany*

[6]*DESY, Hamburg, Germany*

[7]*Helmholtz Zentrum Geesthacht, Geesthacht, Germany*

[8]*SLAC National Accelerator Laboratory, Menlo Park, California 94025, USA*

(Received 1 July 2015; published 21 October 2015)

The time evolution of the electron structure is investigated in a molybdenum foil heated up to the warm dense matter regime by a femtosecond laser pulse, through time-resolved x-ray absorption near-edge spectroscopy. Spectra are measured with independent characterizations of temperature and density. They are successfully compared with *ab initio* quantum molecular dynamic calculations. We demonstrate that the observed white line in the L_3 edge reveals the time evolution of the electron density of state from the solid to the hot (a few eV) and expanding liquid. The data indicate a highly nonequilibrated state, 5 ps after heating.

DOI: 10.1103/PhysRevB.92.144201 PACS number(s): 52.50.Jm, 61.05.cj, 71.22.+i, 78.47.J−

The study of warm dense matter (WDM) has shown a strong renewed interest, due to advances in transient techniques to create matter in this regime [1–6], and in first principles calculations to simulate the physical properties [7,8] involved in various physical domains such as planetary physics [9], inertial confinement fusion [10], and applied laser processes [11]. The difficulty of modeling comes from the atomic level: disordered matter, partially degenerate electrons, and strongly coupled ions. In most situations, *ab initio* quantum molecular dynamic (QMD) simulations are required, considering both the ion spatial distribution through molecular dynamics and the near-continuum electron structure through density functional theory (DFT). DFT is the cornerstone of calculations of most physical properties (equations of state, transport coefficients, etc.). Valuable experimental data are needed to support the constant improvements of numerical codes [12].

In principle, x-ray absorption near-edge spectroscopy (XANES) provides access to the electronic structure, since it probes near-continuum unoccupied states from core levels. Alternatively, x-ray emission spectroscopy (XES) has been proposed to probe the corresponding occupied states [13]. Yet little data are available. The first were obtained near the K edge of warm dense aluminum. At solid density and above, the near free electron gas density of states (DOS) was essentially unchanged. The main modifications observed in the XANES spectra concerned the K-edge shift associated with the change in the core-level screening [14]. During expansion below the solid density, in contrast, the electron DOS was progressively modified during the metal-nonmetal transition, and was revealed by a pre-edge peak in XANES spectra [15,16]. In another study, the metallization of warm dense silica at high temperature has been diagnosed by the Si K-edge shift from the bottom of the valence band (insulator) down to the Fermi energy (semimetal) [17]. Time-resolved XANES (TR-XANES) measurements have also been reported on warm dense copper (noble metal). They were used to retrieve the temporal evolution of the electronic temperature through comparison to theoretical calculations [18], and to address the electron-ion equilibration dynamics in rapidly heated matter.

In this paper, we present a TR-XANES study of femtosecond laser-heated molybdenum. This last has been chosen as a prototype transition metal. Their near-continuum electron structure is dominated by a d band that plays a key role in their physical properties. The white line observed in the L_3-edge spectra is used to reveal the rapid time evolution of the electron DOS. Spectra are measured with independent control of the temperature and density, and they are successively compared with *ab initio* QMD calculations. The experimental data suggest a nonequilibrium state in the first picoseconds, where the DOS is still solid-state-like while the electron temperature reaches several eV.

The principle of the XANES measurement is presented in Fig. 1(a). Spectral features near the Mo L_3 edge are dominated by photoabsorption that couples the $2p_{3/2}$ core level with vacant $4d$ states above the Fermi energy E_F. As the $4d$ band is highly localized in energy, a strong absorption peak also called the white line (WL) is expected. This WL is conventionally interpreted as resulting from the unoccupied electron DOS in condensed matter [19]. We further demonstrate that the WL directly reveals the electron DOS spectral shape, in a large thermodynamical domain from solid to WDM.

The experiment has been performed at the Matter in Extreme Conditions (MEC) instrument at the Linac Coherent Light Source (LCLS). The experimental setup and the XANES measurement procedure have been previously described [20]. A 100 nm thick Mo sample deposited on a 100 μm thick plastic substrate, and covered by an 8 nm layer of amorphous carbon,

*dorchies@celia.u-bordeaux1.fr

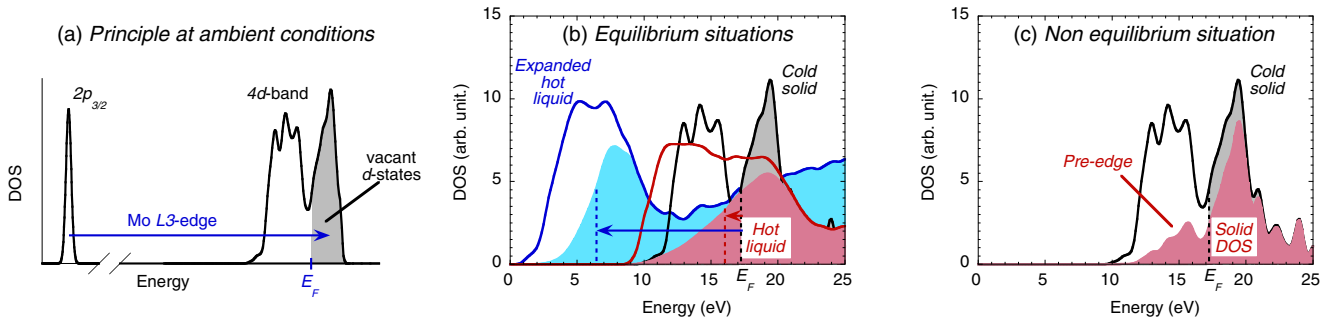

FIG. 1. (Color online) (a) Principle of L_3-edge XANES as a probe of the Mo $4d$ band. (b) Electronic density of states (DOS) from QMD calculations, for three representative situations (solid lines): cold solid, $\rho = 10.12$ g/cc, $T_e = T_i = 300$ K; hot liquid, $\rho = 9.56$ g/cc, $T_e = T_i = 20\,000$ K; expanded hot liquid, $\rho = 5$ g/cc, $T_e = T_i = 10\,000$ K. The respective unoccupied states responsible for the observed Mo L_3-edge white line are indicated with solid areas drawn below the full DOS. Dotted lines: Corresponding Fermi energies. (c) Total and unoccupied DOS when considering the nonequilibrium situation: $\rho = 10.12$ g/cc (solid), $T_i = 300$ K (cold lattice), and $T_e = 20\,000$ K (hot electrons).

is heated by a femtosecond laser pulse (300 fs, 4 J/cm^2, p polarized at 800 nm) at 12° incidence angle. It is probed at different delays by the ultrashort x-ray pulse delivered by the LCLS. The synchronization has been monitored during the experiment, by using the plasma switch method [21], providing $\leqslant$1 ps temporal jitter. For each delay, about 20 successive shots are accumulated in order to obtain a XANES spectrum with a few percent noise level.

The thermodynamic conditions of the sample have been determined by using the one-dimensional (1D) Lagrangian code ESTHER [22]. The laser absorption is calculated by solving the Helmholtz equations. The time evolution is described by hydrodynamics coupled to a two-temperature (electron and ion) multiphase equation of state [23], with consistent ion heat capacity. The electron-ion energy transfer is described by the electron-phonon coupling factor taken from Lin *et al.* [24]. The thermal equilibrium is reached in 2 ps. In the first picoseconds, the Mo layer density remains close to that of the solid. After ~20 ps, because of the high induced pressure, the sample significantly expands, leading to a simultaneous decrease of both temperature and density. At long delays, a portion of the sample expands (laser side), while the other part is slightly constrained by the plastic substrate.

In order to constrain the hydrodynamic simulations, an independent experiment has been performed on the Eclipse laser facility at the CELIA laboratory, using the same samples and similar laser parameters with a fluence varied from 2 to 10 J/cm^2. Fourier domain interferometry has been used as a standard technique to determine the surface velocity [25]. A good agreement is found ($\leqslant$20%) with hydrodynamic simulations. Densities and temperatures corresponding to the delays of XANES measurements are reported in Fig. 2. Data are averaged along the Mo layer thickness and the inhomogeneities are reported in the error bars (standard deviations). At a short delay (several ps), we probe a near solid density at $21\,500 \pm 9500$ K. At longer delays (up to 2 ns), the sample is still hot (~10 000 K), but the density drops to a few g/cc. The conditions considered for QMD simulations, representative of the experiment, are also reported in Fig. 2.

Some characteristic Mo L_3-edge XANES spectra are reported in Fig. 3. They are dominated by a white line with a ~5 eV width. Its amplitude and spectral shift are plotted in Fig. 4 as a function of the delay. In the first picoseconds after heating, the WL amplitude is decreased to 85 ± 5%, then increases slightly to reach ~90% of the cold value at longer delays (~1 ns). The evolution of the spectral shift is not as fast. It takes a few 100 ps to reach a maximal value of -1.10 ± 0.15 eV. The time scales of the temperature and density evolution (cf. Fig. 2) suggest that the WL amplitude decrease could be associated with the fast temperature increase, while the WL negative spectral shift could result from the slower density decrease. Among all the experimental data, the spectrum registered at 5 ps is the only one to present a pre-edge structure, just before the WL. Note that it significantly emerges from the cold WL outside the experimental uncertainty [20].

To simulate molybdenum at a given thermodynamic state, we perform molecular dynamics simulations using the *ab initio* plane wave density functional theory (DFT) code ABINIT [26,27]. DFT is applied together with the generalized gradient approximation [28]. Simulations are performed in the framework of the projected augmented wave (PAW) method [29,30] using a PAW data set including semicore states which

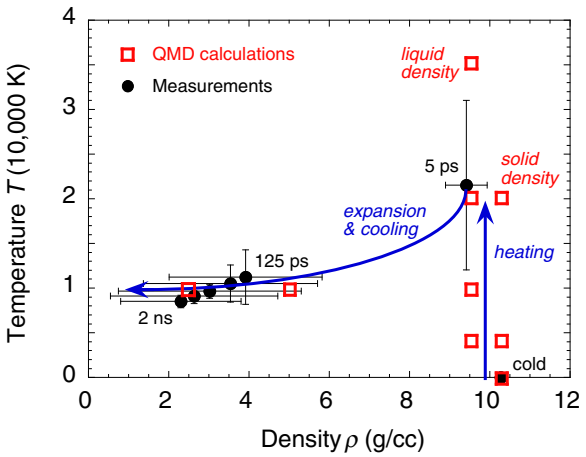

FIG. 2. (Color online) Summary of warm dense Mo density and temperature conditions studied in this paper.

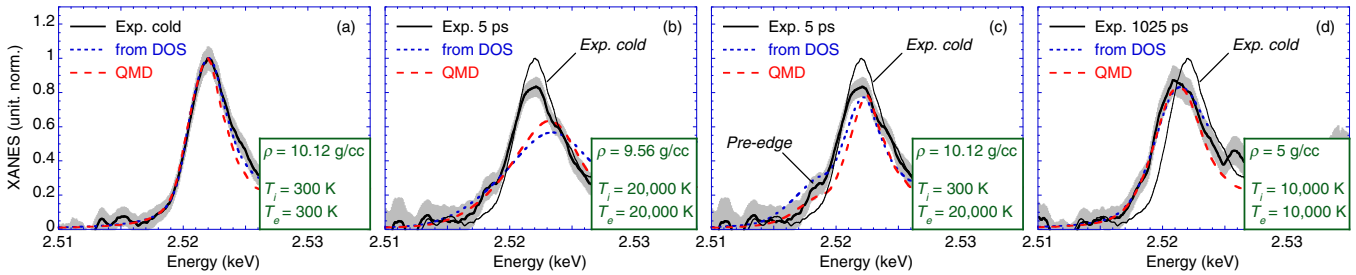

FIG. 3. (Color online) Some representative XANES spectra measured before the laser heating [(a) cold], just after heating when the sample is supposed to be hot and still near solid density [(b), (c) 5 ps time delay] and at a longer time during hydrodynamic expansion that reduces both the temperature and density [(d) 1025 ps time delay]. Measurements (solid lines) are compared with simple calculations from the electron DOS (dotted lines), and with full QMD calculations (dashed lines). The measurement uncertainty is illustrated by the gray area. The spectrum observed for the cold sample is reported as a reference (thin line). The values of density and temperature used for the calculations are indicated in the respective plots. The calculation considers equilibrated temperatures in (a), (b), and (d), and a nonequilibrium situation in (c).

has been benchmarked extensively against physical properties obtained from experiments [31]. The PAW data set is generated with 14 outer electrons ($4s^2 4p^6 4d^5 5s^1$).

To reproduce the Mo L_3-edge white line, a first approach consists in performing an *ab initio* calculation of the absorption cross section following the methodology described in Ref. [32] (more details are given in the Supplemental Material [33]). A second analytical approach is considered, based on the simple picture presented in Fig. 1(a). The electron d DOS obtained from *ab initio* calculations is multiplied by $[1 - f(E)]$, where E is the energy and $f(E)$ is the Fermi-Dirac occupation factor depending on the electronic temperature T_e. The resulting unoccupied DOS is then convoluted by a Lorentzian function that reflects the $2p_{3/2}$ core-hole lifetime. Its width is 1.56 eV full width at half maximum (FWHM), as obtained from an atomic configuration-average calculation [34]. The two calculated spectra are compared to the experiment in Fig. 3(a), considering the case of cold solid Mo. A very good agreement is obtained, validating the WL as a direct diagnostic of the $4d$-band DOS.

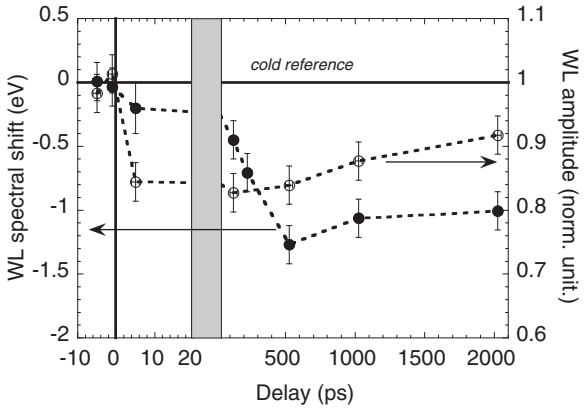

FIG. 4. Evolution of the Mo L_3-edge white line (WL) as a function of time delay after heating. The delay scale (x axis) has been broken in order to highlight the different temporal behaviors of both the amplitude (decrease of ∼15% in the first picoseconds) and the negative spectral shift (more gradual and occurring over a few 100 ps). The spectral shift is defined by the half-height position of the WL rising edge.

The electron DOS has been calculated by QMD for all conditions reported in Fig. 2. Some representative results are plotted in Fig. 1(b). The cold solid exhibits a structured $4d$ band, mainly composed of two separate energy regions. The first one is filled up to the Fermi energy (occupied states). The second one is empty (unoccupied states resulting in the WL). The Fermi level is located in the deep minimum, which is a characteristic feature of bcc transition metals. The $4d$-band envelope is significantly affected when the temperature increases. The structures disappear to form a fairly flat and slightly broadened band, as illustrated in the calculation performed at 20 000 K. Such behavior is observed at temperatures as low as 4000 K, confirming that it is highly correlated with the transition from a solid to a liquid phase, as previously reported in photoelectron spectroscopy measurements [35,36]. The decrease in density results in a negative energy shift of both the $4d$ band and the Fermi energy E_F. The shift of E_F is −1.0 eV when going from solid (10.12 g/cc) down to liquid density (9.56 g/cc), then the shift reaches −10.5 and −15.8 eV at 5 and 2.5 g/cc.

These electronic DOS changes result in a modification of the XANES spectra. Both calculations (WL estimated from the DOS and QMD full XANES simulations) are compared with experimental data in Fig. 3. The DOS blurring and broadening occurring at high temperatures result in a decrease of the WL amplitude. The level of this decrease fits well with the observations at relatively long delays ($\gtrsim$100 ps when the temperature is close to 10 000 K). The agreement is less satisfactory at the shortest delay (5 ps), which will be discussed.

The DOS energy shift with the density results in a WL energy shift, but a proper calculation requires additional information about the core-level energy ($2p_{3/2}$) that is also modified with the density, since the atomic potential screening is affected. The core-level shift cannot be directly calculated by the QMD simulations, in which only the 14 outer electrons are explicitly treated. Therefore, a calculation has been performed using the DFT WIEN2K code, taking explicitly into account all the electrons in the Mo electronic cloud [37] (see the Supplemental Material for more details). Both the $2p_{3/2}$ energy level and E_F are predicted to linearly decrease when the density decreases from the solid to a few g/cc, before converging towards the isolated atom values (below 1 g/cc). Consequently, the E_F decrease is mainly compensated by the

core-level shift. From the solid down to the liquid density, this results in a quasiunmodified energy position for the WL, in agreement with the measurements at the shortest delays. At 5 and 2.5 g/cc, residual WL energy shifts of ~ -0.9 and ~ -1.8 eV are predicted by the calculations, in close agreement with the spectra measured at the longest delays [cf. Fig. 3(d)].

The L_3-edge Mo XANES spectra are well reproduced by both calculation approaches (except the measurement at 5 ps). This agreement confirms that the observed WL modifications can be interpreted in the whole density-temperature domain explored in this study, in terms of associated DOS changes: (i) The WL amplitude decrease reveals the DOS blurring when the temperature increases, and (ii) the WL negative shift is due to the DOS energy shift when the density decreases.

The spectrum registered at the shortest delay (5 ps) exhibits a pre-edge structure. In Fig. 3(b), we report calculations performed at 20 000 K and liquid density (expected average conditions at 5 ps, cf. Fig. 2). They show a WL amplitude decrease significantly stronger than observed, as well as a broad slope in the rising edge due to the temperature dependence of $f(E)$. This is clearly different from the pre-edge observed in the experiment. The XANES spectrum measurement could be affected by the large temperature gradient as a function of the depth expected at short delays. By considering a deliberately extreme situation (half of the Mo layer at 300 K, and the other half at 35 000 K), the average XANES spectrum remains similar to the one calculated at 20 000 K, and does not result in a pre-edge. A satisfactory agreement is found, if we consider a nonequilibrium situation where the electronic temperature is $T_e = 20\,000$ K, while the DOS is still structured as in the cold solid [cf. Fig. 3(c)]. The corresponding unoccupied DOS is plotted in Fig. 1(c). The increase in T_e promotes some electrons from the first energy region (initially full) to the second one (initially empty). That results in a peak pattern in the unoccupied DOS just below E_F, responsible for the pre-edge structure observed in the XANES spectrum. A similar feature has been observed in previous calculations, when increasing the ionization state of bcc Mo [38].

Such a nonequilibrium situation is unexpected as late as 5 ps after heating. The electron DOS is supposed to adapt very rapidly to the atomic spatial distribution (on a femtosecond time scale). If we consider that the sample transforms into a hot liquid as soon as the ionic temperature exceeds the melting temperature, then the time scale should be even shorter than the electron-ion thermal equilibration estimated to be achieved in 2 ps [24]. Recent papers suggest that the electron-ion coupling could be reduced in the WDM regime, which would lead to longer equilibration times [39,40]. Previous studies suggested that a hot electron population (a few eV's) could strengthen the lattice stability and thus delay the melting time [41,42]. This is expected for some noble metals, but not for transition metals such as molybdenum [43]. A final possibility is that an additional delay is needed for the atomic spatial distribution to change after the melting temperature is reached, or because of hydrodynamic effects.

In summary, we present time-resolved XANES spectra measured near the L_3 edge of a molybdenum foil rapidly heated by a femtosecond laser pulse. The hydrodynamic expansion has been carefully estimated from calculations and optical measurements. Just after heating, the warm dense molybdenum temperature reaches a few eV at near solid density. Then, the density progressively decreases down to a few g/cc. XANES spectra are dominated by a white line whose shape and time evolution are successively reproduced by *ab initio* QMD calculations. We demonstrate that it can be directly interpreted in terms of the unoccupied electron DOS near the continuum. From this study, we deduce that the electron DOS is blurred and broadened when the temperature increases beyond melting. When the density decreases, the DOS shifts towards low energies. In the XANES spectra, this last effect is partially compensated by the $2p_{3/2}$ core-level energy shift due to the change in screening. At the shortest time delay (5 ps), the observed XANES spectrum suggests a nonequilibrium situation (a high electron temperature $\sim$2 eV, but still solid-state-like electron DOS). Further experimental studies are needed to find out the details of such a nonequilibrium persistence during the ultrafast transition from solid to WDM.

This work was supported by the French Agence Nationale de la Recherche, under Grant OEDYP (ANR-09-BLAN-0206-01) and Programme IdEx Bordeaux - LAPHIA (ANR-10-IDEX-03-02), and by the GENCI program providing computational time under the Programs GEN6046 and GEN6454. The authors gratefully acknowledge Benoit Chimier and Olivier Peyrusse for fruitful discussions respectively concerning hydrodynamic simulations and XANES spectra calculations, Rodrigue Bouillaud and Laurent Merzeau for their technical assistance, and Frédéric Burgy and Fanny Froustey for laser operation at CELIA. The authors thanks Marc Torrent for his great help with ABINIT simulations. B.I.C. acknowledges support from the National Research Foundation of Korea (NRF-2013R1A1A1007084, NRF-2015R1A5A1009962) and the TBP research project of GIST. Portions of this research were carried out at the Linac Coherent Light Source (LCLS) at the SLAC National Accelerator Laboratory. LCLS is an Office of Science User Facility operated for the U.S. Department of Energy Office of Science by Stanford University. The MEC instrument has additional support from the DOE Office of Science, Office of Fusion Energy Sciences under Contract No. SF00515.

[1] M. Koenig, B. Faral, J. M. Boudenne, D. Batani, A. Benuzzi, S. Bossi, C. Remond, J. P. Perrine, M. Temporal, and S. Atzeni, Phys. Rev. Lett. **74**, 2260 (1995).

[2] G. W. Collins, L. B. Da Silva, P. Celliers, D. M. Gold, M. E. Foord, R. J. Wallace, A. Ng, S. V. Weber, K. S. Budil, and R. Cauble, Science **281**, 1178 (1998).

[3] M. D. Knudson, D. L. Hanson, J. E. Bailey, C. A. Hall, J. R. Asay, and W. W. Anderson, Phys. Rev. Lett. **87**, 225501 (2001).

[4] P. K. Patel, A. J. Mackinnon, M. H. Key, T. E. Cowan, M. E. Foord, M. Allen, D. F. Price, H. Ruhl, P. T. Springer, and R. Stephens, Phys. Rev. Lett. **91**, 125004 (2003).

[5] K. Widmann, T. Ao, M. E. Foord, D. F. Price, A. D. Ellis, P. T. Springer, and A. Ng, Phys. Rev. Lett. **92**, 125002 (2004).
[6] A. Lévy *et al.*, Phys. Plasmas **22**, 030703 (2015).
[7] D. Hohl, V. Natoli, D. M. Ceperley, and R. M. Martin, Phys. Rev. Lett. **71**, 541 (1993).
[8] S. Mazevet and G. Zérah, Phys. Rev. Lett. **101**, 155001 (2008).
[9] T. Guillot, Science **286**, 72 (1999).
[10] J. Lindl, Phys. Plasmas **2**, 3933 (1995).
[11] J. W. Chan, T. Huser, S. Risbud, and D. M. Krol, Opt. Lett. **26**, 1726 (2001).
[12] National Research Council, *Frontiers in High Energy Density Physics: The X-Games of Contemporary Science* (National Academic Press, Washington, D.C., 2003).
[13] S. M. Vinko *et al.*, Phys. Rev. Lett. **104**, 225001 (2010).
[14] A. Benuzzi-Mounaix *et al.*, Phys. Rev. Lett. **107**, 165006 (2011).
[15] F. Dorchies *et al.*, Phys. Rev. Lett. **107**, 245006 (2011).
[16] A. Lévy *et al.*, Phys. Rev. Lett. **108**, 055002 (2012).
[17] A. Denoeud *et al.*, Phys. Rev. Lett. **113**, 116404 (2014).
[18] B. I. Cho *et al.*, Phys. Rev. Lett. **106**, 167601 (2011).
[19] *X-ray Absorption: Principles, Applications, Techniques of EXAFS, SEXAFS and XANES*, edited by D. C. Koningsberger and R. Prins (Wiley, New York, 1988).
[20] J. Gaudin *et al.*, Sci. Rep. **4**, 4724 (2014).
[21] M. Harmand *et al.*, J. Instrum. **7**, P08007 (2012).
[22] J.-P. Colombier, P. Combis, F. Bonneau, R. Le Harzic, and E. Audouard, Phys. Rev. B **71**, 165406 (2005).
[23] A. V. Bushman, I. V. Lomonosov, and V. E. Fortov, Sov. Tech. Rev. B: Therm. Phys. **5**, 1 (1993).
[24] Z. Lin, L. V. Zhigilei, and V. Celli, Phys. Rev. B **77**, 075133 (2008). Mo data are available online on www.faculty.virginia.edu/CompMat/electron-phonon-coupling/
[25] F. Deneuville, B. Chimier, D. Descamps, F. Dorchies, S. Hulin, S. Petit, O. Peyrusse, J. J. Santos, and C. Fourment, Appl. Phys. Lett. **102**, 194104 (2013).
[26] X. Gonze *et al.*, Comput. Phys. Commun. **180**, 2582 (2009).
[27] F. Bottin, S. Leroux, A. Knyazev, and G. Zerah, Comput. Mater. Sci. **42**, 329 (2008).
[28] J. P. Perdew, K. Burke, and M. Ernzerhof, Phys. Rev. Lett. **77**, 3865 (1996).
[29] P. E. Blöchl, Phys. Rev. B **41**, 5414 (1990).
[30] M. Torrent, F. Jollet, F. Bottin, and G. Zerah, Comput. Mater. Sci. **42**, 337 (2008).
[31] A. Dewaele, M. Torrent, P. Loubeyre, and M. Mezouar, Phys. Rev. B **78**, 104102 (2008).
[32] V. Recoules and S. Mazevet, Phys. Rev. B **80**, 064110 (2009).
[33] See Supplemental Material at http://link.aps.org/supplemental/10.1103/PhysRevB.92.144201 for details about *ab initio* quantum molecular dynamic calculations.
[34] O. Peyrusse, J. Phys. B **32**, 683 (1999).
[35] P. Oelhafen, R. Wahrenberg, and H. Stupp, J. Phys.: Condens. Matter **12**, A9 (2000).
[36] H. Stupp, H. G. Boyen, G. Gantner, and P. Oelhafen, J. Non-Cryst. Solids **270**, 1 (2000).
[37] P. Blaha *et al.*, *WIEN2k, An Augmented Plane Wave + Local Orbitals Program for Calculating Crystal Properties* (Karlheinz Schwarz, Techn. Univ. Wien, Austria, 2001).
[38] F. M. F. de Groot, Z. W. Hu, M. F. Lopez, G. Kaindl, F. Guillot, and M. Tronc, J. Chem. Phys. **101**, 6570 (1994).
[39] Z. Chen, B. Holst, S. E. Kirkwood, V. Sametoglu, M. Reid, Y. Y. Tsui, V. Recoules, and A. Ng, Phys. Rev. Lett. **110**, 135001 (2013).
[40] P.-M. Leguay *et al.*, Phys. Rev. Lett. **111**, 245004 (2013).
[41] V. Recoules, J. Clerouin, G. Zerah, P. M. Anglade, and S. Mazevet, Phys. Rev. Lett. **96**, 055503 (2006).
[42] R. Ernstorfer, M. Harb, C. T. Hebeisen, G. Sciaini, T. Dartigalongue, and R. J. Dwayne Miller, Science **323**, 1033 (2009).
[43] E. Bevillon, J. P. Colombier, V. Recoules, and R. Stoian, Phys. Rev. B **89**, 115117 (2014).